Temporal-spatial modeling of electron density enhancement due to successive lightning strokes

Erin H. Lay[(1)] , Craig J. Rodger[(2)], Robert H. Holzworth[(3)], Mengu Cho[(4)], and Jeremy N. Thomas[(3,5)]

(1) Los Alamos National Laboratory, Los Alamos, NM

(2) University of Otago, Dunedin, New Zealand

(3) Dept. of Earth and Space Sciences, University of Washington, Seattle, WA

(4) Department of Electrical Engineering, Kyushu Institute of Technology, Japan

(5) Dept. of Electrical and Computer Eng., Digipen Institute of Tech., Redmond, WA

Abstract. We report results on the temporal-spatial modeling of electron density enhancement due to successive lightning strokes. Stroke rates based on World Wide Lightning Location Network (WWLLN) measurements are used as input to an axi-symmetric Finite Difference Time Domain (FDTD) model that describes the effect of lightning electromagnetic pulses (EMP) on the ionosphere. Each successive EMP pulse interacts with a modified background ionosphere due to the previous pulses, resulting in a non-linear electron density perturbation over time that eventually reaches a limiting value. The qualitative ionospheric response to successive EMPs is presented in two-dimensional, axi-symmetric space. Results from this study show that the non-linear electron density perturbations due to successive lightning strokes must be taken into account and varies with altitude. The limiting maximum electron density is reached

earlier in time for higher altitudes, and the most significant effect occurs at 88 km. The limiting modeled electron density profile in the 83 to 91 km altitude range does not depend on the initial electron density.

Introduction

The electromagnetic pulse (EMP) from lightning has been shown to modify conductivity and electron density in the lower ionosphere [Mende et al., 2005, Cheng and Cummer, 2005]. Transient luminous events (TLE) are evidence of lightning energy coupling with the lower ionosphere via quasi-electrostatic as well as electromagnetic fields, and can cause ionization, heating and optical emissions in the lower ionosphere [Inan et al., 1991, Tarenenko et al., 1993, Fukunishi et al., 1996, Pasko et al., 1997].

One particular type of TLE called elves is caused by the lightning EMP that expands outward from a high-peak-current (>50 kA) cloud-to-ground stroke [Barrington-Leigh and Inan, 1999]. When the EMP reaches an altitude of 85-95 km, its electric field interacts with the ionospheric plasma causing optical excitation and secondary ionization. The elves themselves are the optical emissions, which appear to expand in a ring shape that can be as large as 700 km in diameter and last 1 to 3 ms [Barrington-Leigh and Inan 1999]. Mende et al. [2005] have reported enhanced electron density of 210 electrons cm^{-3} in a 165 km diameter region in which there was a detected optical emission from an elve. Rodger et al. [2006] have conservatively estimated that the EMP associated with elves could impact >1% of the surface area of the lower ionosphere per minute. These observations and calculations indicate that the EMP from strong lightning strokes could create enhanced electron density over a large region of the lower ionosphere. Ionization and attachment caused by the EMP are the focus of this study.

Given that making in situ measurements of lightning-driven fields in the lower ionosphere is very difficult, and has only been accomplished a handful of times [e.g., Holzworth et al., 1985, Kelley et al., 1997], models of the interaction between the

lightning stroke and the lower ionosphere can be illuminating. Various models predict this interaction and are consistent with optical observations of TLEs [Taranenko et al., 1993; Fernsler and Rowland, 1996; Pasko et al., 1997; Marshall et al., 2008; Cho and Rycroft, 1998, 2001]. These models indicate that lightning EMP causes electron heating, ionization, and dissociative attachment of the lower ionosphere that affect the local conductivity and electron density. It has also been proposed that in severe thunderstorms with high flash rates of strong lightning strokes, the time between flashes could be smaller than the decay time for ionization changes of 10-100 s [Mika and Haldoupis, 2008], allowing lightning-induced electron density increases to accumulate locally in the lower ionosphere [Barrington-Leigh and Inan, 1999].

In the work of Taranenko et al. [1993], a 1-D model was used to show significant modifications in the electron density at altitudes of 75 to 95 km. This work provided initial evidence of non-linear response to multiple lightning strokes by applying an electromagnetic pulse that was 20 times as long in duration as the pulse for a single stroke, and noting that the maximum change in electron density was not 20 times larger than that of a single stroke. The work of Rodger et al. [2001] also studied the accumulation of EMP effects on the lower ionosphere by using the electromagnetic model developed in Cho and Rycroft [1998]. In their work, Rodger et al. [2001] predicted a possible 100% to 900% increase in electron density in the 88 to 92 km altitude range for a period of more than an hour due to accumulated EMP effects of NLDN-located lightning. However, their work did not include the non-linear effect of the EMP interaction with the ionosphere, a weakness noted by these authors. The non-linear effect in this case refers to fact that when one lightning stroke perturbs the electron density in a

certain region, the next lightning stroke will interact in a medium with a different background electron density if not enough time has passed for the electron density to return to its original conditions.

This paper builds on the study of Rodger et al. [2001] by addressing non-linear effect of the lightning EMP/ionosphere interaction as mentioned above by using the Cho and Rycroft [1998] model, with a few modifications, to describe the accumulated effect of strong lightning strokes on the nighttime lower ionosphere. We also build on the work of Taranenko et al. [1998] by accounting for the electron density relaxation that occurs between lightning strokes, as well as by providing a 2-D prediction of electron density perturbations due to successive lightning strokes. We also demonstrate that the time required to reach a limiting electron density value is altitude-dependent.

The authors of this work have chosen to use data from the World-Wide Lightning Location Network (WWLLN) [Dowden et al., 2002, Rodger et al., 2006, Lay et al., 2006] because of its ability to monitor the global impact of lightning EMP. We hope to be able to extend the impacts of this work to monitor ionospheric regions with potential perturbations on a global scale based on WWLLN global coverage. The work of Rodger et al. [2006] shows that ~75% of WWLLN strokes have peak current >50 kA. Based on a study of NLDN-detected cloud-to-ground (CG) lightning [Barrington-Leigh and Inan, 1999] that found that all lightning with peak current >55 kA produced elves, while ~70% of lightning with peak current >45 kA produced elves, it is estimated that ~75% of WWLLN-detected lightning could produce elves. With this global coverage of elves-producing strokes, one could extend modeled spatial and temporal perturbations based on WWLLN stroke rates to a global scale. The number of lightning detected by WWLLN in

2008 was 54.4 million strokes [Rodger et al., 2009]. Multiplying this number by 75% and dividing by the number of minutes in a year, we determine a 2008 WWLLN elves-producing-lightning detection rate of 78 per minute, or 37% of the estimated total elves-producing lightning rate of 210 per minute from the work of Rodger et al. [2006]. Because of the WWLLN capability of monitoring global lightning EMP from high peak current lightning strokes and the goal of extending spatial-temporal perturbation monitoring to a global scale, we have used WWLLN lightning stroke rates in the simulation to be described below.

Model Formulation

The Cho and Rycroft [1998] model is a 2-dimensional axi-symmetric model used in this paper to predict the interaction of the EMP radiated by lightning with the nighttime lower ionosphere. In this model, a vertical lightning stroke is placed at the origin and a Finite Difference Time Domain (FDTD) technique then is used to propagate the electromagnetic field in time and 2-dimensional space. The electric field interacts self-consistently with the electrons in the ionosphere, causing dissociative attachment, optical emission, and ionization when the electric field surpasses given thresholds. The collision frequency used in the model is determined via an electric-field-dependent mobility. Although we focus on EMP effects in this paper, the model also includes the quasi-electrostatic effect that is due to the relocation of charge during the return stroke process. However, these effects are lower in altitude (65-80 km), where decay times of perturbed electron density are shorter and where the overall electron density is lower by 1 to 3 orders of magnitude.

The lightning discharge current density profile is discussed in Cho and Rycroft, [1998], and will not be reproduced here. The current density profile can be integrated in the horizontal direction to describe the lightning current pulse used in the model:

$$I(z=0,t) = Q\frac{1}{12}\frac{1}{\tau}\left(\frac{t}{\tau}\right)\exp\left(-\left(\frac{t}{\tau}\right)^{1/2}\right), \quad (1)$$

where Q is the total charge transferred, and τ is a characteristic time constant.

The background electron density is not well known at any particular time, and has a significant impact on the magnitude of the electric field as it penetrates the ionospheric medium. The ambient electron density profile used in the work of Cho and Rycroft [1998] is given by:

$$\begin{aligned} n_e(z) &= 8.0 \text{ x } 10^{-4} e^{(z/4.3 \text{ km})} \text{ (cm}^{-3}\text{)}, \; z \leq 105 \text{ km} \\ n_e &= n_e(z = 105 \text{ km}), \; z > 105 \text{ km} \end{aligned} \quad (2)$$

In this study, the ambient electron density profile used in the Cho and Rycroft [1998] model was replaced with the electron density profile proposed by Wait and Spies [1964] (hereafter referred to as the "Wait profile") because the Wait profile has been experimentally determined to correlate well with data [Thomson, 1993; McRae and Thomson, 2000]. The Wait electron density profile is given by:

$$n_e(z) = 7.857 \text{ x } 10^{-5} e^{\beta(z-H')} \nu(z) \text{ (cm}^{-3}\text{)}, \quad (3)$$

where z is the altitude, β is a parameter of "steepness" of the ionospheric profile (β = 0.5 has been determined for nighttime ionosphere) [Ferguson and Snyder, 1987], H' is 85 km for a nighttime ionosphere, and $\nu(z)$ is the ambient collision frequency given by:

$$\nu(z) = 1.86 \text{ x } 10^{11} e^{-0.15z} \text{ (s}^{-1}\text{)}. \quad (4)$$

Since only instruments on rockets can make in situ measurements of ionospheric electric fields at the 85 to 95 km altitude range, very few in situ measurements have been

made. However, the work of Thomas et al. [2008] compared in situ ac and dc rocket-measured electric field data from an ionospheric rocket flight launched from Wallops Island, VA on 2 September 1995 [Barnum, 1999; Kelley et al., 1997; Thomas et al., 2008] with the 2D-EMP model of Cho and Rycroft [1998]. In the work of Thomas et al. [2008], the rocket-measured electric fields at 90 km altitude and 260 km from the corresponding lightning stroke were compared to modeled electric fields in the same location from the Cho and Rycroft [1998] model. This finding suggests that the EMP model of Cho and Rycroft overestimates the magnitude of the lightning-driven electric fields measured by the rocket in this case. One explanation for this overestimation could be that conductivity of the ionosphere during the rocket flight was much higher than assumed, causing these electric fields to be attenuated much more quickly than predicted by the 2D-EMP model. Their finding indicates that background electron density may be important in the model predictions.

Relaxation of enhanced electron density

The 2D-EMP code simulates the 2 ms following a lightning stroke, during which the EMP of the lightning stroke is propagated to the lower ionosphere. After the 2 ms time window, the EMP has passed through the region, and the resultant perturbed electron density undergoes recombination (capture of an electron by a positive ion) and attachment (electron capture by neutral molecule) in a return to the original steady state electron density. A numerical solution has been determined by using a 4^{th} order Runge-Kutta method to describe nighttime relaxation of ionospheric electron density perturbations caused by an impulsive sferic. The differential equation used to describe the change in electron density in this simulation is:

$$\frac{\partial N_e}{\partial t} = q - \beta N_e - \alpha N_e^2 \quad \text{[Rodger et al., 1998]}, \tag{5}$$

with q as the nighttime steady-state ionization rate due to cosmic rays and nighttime solar Lyman-α scattered from the geocorona, β as the attachment coefficient, and α as the recombination coefficient. The value of q for steady-state is determined by setting the left-hand side of Equation 5 to zero. The values for α and β are taken from Rodger et al. [1998] in which a simplified ionospheric chemistry model is described. This has been tested against the much more complex Sodankyla Ion Chemistry model [Verronen et al., 2005], and found to give similar results for the steady state electron density [Rodger et al., 2007]. Attachment dominates below 80 km altitude due to high concentrations of cluster ions, and recombination dominates above 85 km altitude due to high concentrations of O_2^+. We used the MSIS-E-90 model to describe the neutral atmosphere (NO, NO_2, O_2, mass density, electron temperature, and neutral temperature) versus altitude [*Hedin*, 1991]. Note that this technique predicts electron density relaxation times based on chemical reaction models, and not the decay times as measured by D-region remote-sensing narrowband amplitude and phase perturbations.

Figure 1 shows the 1/*e* decay time of the electron density enhancement from this relaxation code at different ionospheric altitudes. The relaxation time is the longest at ~88 km. Narrowband VLF transmitters do not probe up to 90 km altitude, so they are unable to give relaxation times at those altitudes. The long life times at 88-90 km altitude are mostly the very weak part of the ionization perturbation slowly fading away. These changes would not be detectable through most D-region remote sensing techniques. The noise floor on the narrow band technique is such that the

long-lived part of the ionization change is unlikely to be detectable. The 88-km altitude is also that at which the EMP has the most significant impact on electron density. If large strokes occur more frequently than the relaxation time of the electron density enhancement, then the enhancement may accumulate over a period of a number of strokes. Subsequent strokes then will interact with a modified ionosphere, and may create non-linear behavior. This non-linear behavior is the focus of this investigation.

Accumulated enhancements due to successive lightning strokes

In the following simulation, the above-described 2D-EMP model predicts the change in electron density due to lightning EMP. The electron density enhancement is then allowed to relax for a time *t* via the above numerical method. Next, the 2D-EMP model simulates a second lightning stroke occurring at a time *t* after the first. The EMP from this second stroke then interacts with the newly modified (and relaxed) ionosphere. This process is repeated nine times to simulate the effect of the EMP from 10 successive lightning strokes upon the same ionospheric region.

Lightning flash rates from a storm detected by the WWLLN centered on 9.0 N, 95.5 W between 3:00 and 7:30 UT on 1 July 2007 are used to determine the time *t* between strokes that will be used in this simulation. We choose this location because it appears to be a region with an unexpectedly high occurrence rate of elves as detected by the ISUAL instrument, possibly due to high sea surface temperatures [Chen et al., 2008]. Chen et al. [2008] calculate that elves (in other words, lightning EMP) could contribute 5% of the free electrons in the Caribbean region. The WWLLN CG detection efficiency of ~4% calculated by Jacobson et al. [2006] for the southeast U.S. is the detection efficiency that has been experimentally calculated nearest to the storm of interest. It is used to estimate a

stroke rate of 2 strokes per second during the peak of the storm for a period of 20 minutes. Note that this detection efficiency may be a lower limit since it was calculated using data from 2004, and the WWLLN has installed additional receiving stations since then [Rodger et al., 2009]. As a lower limit on detection efficiency, it would correspond to an upper limit on stroke rate, and, hence, an upper limit on EMP-produced ionospheric perturbations.

The 2D-EMP simulation results show a minimum peak current of 100 kA in order to produce any increase in electron density in the lower ionosphere. In order to determine the percentage of WWLLN strokes detected that are larger than 100 kA, we look to findings in Golde [1977] and Rakov and Uman [2003] that have been used by Rodger et al. [2005, Figure 6] to approximate a function that describes the probability that a CG lightning stroke (of either polarity) would be larger than a given peak current. By using this cumulative-lightning peak-current probability, we estimate that approximately 5% of all WWLLN-detected strokes have peak currents greater than 100 kA and ~2.5% of all strokes have peak currents greater than 150 kA. Therefore, the estimated stroke rate of 150-kA-or-greater strokes in the given storm is 0.2 s^{-1}, or 1 every 5 seconds. This cutoff is chosen so that half of all strokes that cause electron density enhancements have peak currents larger than 150 kA and half have peak currents less than 150 kA.

For this simulation, we use a 150-kA negative CG stroke with a current pulse of the form given in Equation 1, with τ = 5 microseconds and Q = 16.5 Coulombs. These values for τ and Q were chosen to produce a current waveshape similar in rise and decay times to the first return stroke current waveshape documented in Figure 4.33 of Rakov and Uman [2003]. The -CG stroke excites the ionospheric electron density using the 2D-

EMP simulation, and then the electron density relaxes for 5 seconds via the numerical method described in the previous section before the next 150-kA stroke occurs at the same location. For real lightning locations, subsequent strokes would not occur in exactly the same location, but most probably within the storm region of 30-50 km. This initial simplification is used since we are focused on investigating the non-linear affect of successive strokes. We will extend this method to a more realistic case in the future.

Model Results

Figure 2 shows the steady-state electron density profile (highlighted by a black box on the right side of the top panel), along with the electron density profile after one 150-kA stroke (left side, top panel) and after ten 150-kA strokes (left side, bottom panel), spaced 5 seconds apart. Figure 3 shows the percent change in electron density from steady-state for the same two simulation cases. After one stroke, the maximum change in electron density is 34%, and occurs at 88.5 km altitude and 103 km range. After ten strokes, the maximum percentage change is 295% at an altitude of 87 km and a range of 103 km. The thick white contours represent zero percent change. The space around the region of enhanced electron density actually has a decrease in electron density. The space to the lower, left-hand corner of the gray-colored contour closest to the origin of the lower figure has a decrease in electron density of 50% or more, and is due to fact that the electric field magnitude in that region is dominated by the electrostatic field of the stroke. Decreases in electron density can occur when the electric-field magnitude surpasses the attachment threshold but not the ionization threshold. The only mechanism we have included for an ionization decrease to rise to background levels is the steady-state

ionization due to cosmic rays. We have not included electron detachment in the electron density relaxation equation, but it is possible that detachment could eliminate any resultant electron depletions on a faster time scale than is shown here.

Figure 4 shows the electron density at 92, 90, 88, and 85 km altitude and Figure 5 shows the percentage change in electron density at these altitudes after each successive stroke using this technique. In Figure 4, the dashed-dotted line in each panel shows the electron density after each stroke when using a linear model. The non-linear behavior of the effect of EMP on the medium is clear at all altitudes. At 92 km altitude, the non-linear electron density approaches a limit of ~5.45 $\times$ 10^8 m^{-3}, or about a 13% increase. In contrast, if a linear approach were used, the electron density would increase by 42% over these 10 strokes. The electron density at 90 km seems to approach a limit of ~100% increase more slowly than at 92 km. The increase in electron density at 88 km is very similar to the linear case until after the third consecutive stroke, at which point the two electron density curves diverge. After 10 strokes, the non-linear approach predicts an increase of ~250% at 88 km and as compared to an increase of ~330% with the linear approach. The change in electron density per stroke at 85 km actually increases with the number of successive strokes, such that the non-linear approach predicts a ~50% larger electron density increase than the linear approach. Based on results from 90 and 92 km, one might expect electron densities at 85 and 88 km to reach limits eventually, but they show no sign of converging within these 10 strokes. Over 10 successive strokes using the non-linear modeling, the electron density at 85 km increases by 183%.

An explanation of processes underlying this behavior is the following: the amount of ionization at a particular location due to a lightning stroke is dependent on the magnitude

of the electric field at that location, and electric fields that surpass an ionization threshold increase electron density. However, the magnitude of the electric field is dependent on the conductivity, which is in turn directly dependent on electron density. Because the relaxation times for enhanced electron density are slow, as shown in Figure 1, an electron density enhancement may remain when the next stroke occurs. This enhancement leads to increased conductivity of the medium. As electron density increases, conductivity increases, and the electric field of the wave attenuates more as it passes through the medium. At some point, the medium reaches a limit where conductivity is too high to allow the electric field to penetrate with enough amplitude to reach the ionization threshold, and therefore, the electron density does not increase past that magnitude. At 92 km altitude, the limit seems to be reached at an electron density of ~5.45×10^8 m^{-3}. At 85 km, the rate of electron density increase is actually higher for later strokes than earlier ones. An explanation of this effect is that 85 km is near the lower boundary of the region of electron density enhancement. Below the region of enhancement, a region of decreased electron density develops over successive strokes as shown in Figure 3. The region of decreased electron density below 85 km allows the radiated electric field of subsequent lightning strokes to penetrate to 85 km altitude with less attenuation, and thus produce a larger enhancement than the previous stroke.

In order to investigate the dependence of the model output on the input electron density profile, we ran the 10 successive stroke 2D-EMP model for an initial electron density profile with the parameters H' = 85 km and β = 0.4 km^{-1}, instead of the original profile of H' = 85 km and β = 0.5 km^{-1}. This creates a background electron density profile

with the same characteristic height, but with a less steep increase in electron density versus altitude.

Figure 6 shows a perturbed electron density profile taken vertically at the horizontal range of maximum percentage change after 1 stroke (Figure 6a) and after 10 strokes (Figure 6b) for both the original electron density profile (β = 0.5 km^{-1}; dotted line) and the new electron density profile (β = 0.4 km^{-1}; thick solid line). The thin solid lines represent the initial electron density profiles before perturbation. One can see from Figure 6b that despite the different initial profiles, the perturbed profiles in both cases begin to reach the same electron density in the region between 83 and 91 km altitude. This indicates that the electron density limit in the 83 to 91 km range seems to be independent of initial electron density.

Discussion

From the profiles in Figure 6, we can compare 2D-EMP model results to empirically-based calculations of ionospheric modifications due to lightning from Cheng et al. [2007] that were made using the remote sensing technique presented in Cummer et al. [1998]. This technique detects VLF radiation from lightning strokes which has propagated on a long path, before and immediately after a strong elve-producing lightning stroke which modifies part of the ionosphere along that path. By working with the received VLF spectrum and the LWPC model for ionospheric propagation, the authors iteratively recover the parameters *H'* and β for a Wait electron density profile in the VLF propagation path following the technique presented in Cheng and Cummer, [2005]. Using this technique, Cheng et al. [2007] found a background Wait electron

density profile with values of H'=85 km and β=0.4 km^{-1} immediately before an elve-producing lightning stroke. The error in their method is estimated at 0.2 km in H' and 0.01 km^{-1} in β [Cummer et al., 1998]. Cheng et al. [2007] also statistically analyzes the effects on lower ionospheric electron density of 27 lightning strokes with peak current >60 kA.

Figure 4a of Cheng et al. [2007] presents a perturbed electron density profile associated with an elve-producing lightning stroke estimated by the NLDN to have -106 kA peak current. They find that this lightning stroke causes an enhancement in electron density between 88 and 96 km altitude, with a 2-fold increase at ~92 km. It also creates a decrease in electron density between 78 and 88 km, with a 5-fold decrease at ~82 km. Figure 4b of Cheng et al. [2007] presents an averaged perturbed profile for the 27 averaged lightning strokes with mean peak current -79 kA. They find that these strokes cause an average enhancement in electron density between 83 and 95 km altitude, with a 2-fold increase at ~88 km. These strokes also create an average decrease in electron density between 75 and 83 km, with a 1.5-fold decrease at ~80 km.

The background profile of the solid line in Figure 6a is the same as the background profile in Figure 4b of Cheng et al. [2007], and the perturbed profile in Figure 6a of our paper (after one modeled -150 kA stroke) is similar to the profile (in terms of regions and magnitudes of increase and decrease) for the averaged strokes of -79 kA presented in Figure 4b of Cheng et al. [2007]. This signifies that the model presented in our paper may underestimate the perturbed change in electron density for a lightning stroke of a given peak current. In Figure 6a above, the perturbation from a single -150 kA stroke is similar in magnitude to the experimentally-determined perturbation for strokes with an average

peak current of -79 kA. The perturbed profile in Figure 6b (10 successive modeled -150 kA strokes) is slightly larger in magnitude than the perturbation due to one elve-producing lightning stroke shown in Cheng et al. [2007] Figure 4a. Also, after 10 strokes, the modeled electron density enhancement has moved lower in altitude than that shown in Figure 4a of Cheng et al. [2007], which is consistent with the findings presented above that successive lightning strokes effectively move the region of enhanced electron density lower in altitude as the electron density at higher altitudes reaches a limiting amount.

In the following paragraphs, we discuss some of the remaining uncertainties that could be producing these discrepancies between the empirically-based calculations of electron density perturbations and the 2D-EMP modeled results. Peak currents estimated by the NLDN are noted to have uncertainties of at least 20% to 30% [Cummins et al., 1998], and makes use of an empirical formula which has only been tested out to 60 kA [Orville, 1999]. This uncertainty could modify the 2D-EMP estimate of electron density enhancement by a factor of 3 due to a change in magnitude of radiated electric field from the lightning stroke. Another source of error is the description of the lightning stroke current pulse. By narrowing the pulse in this EMP model, *di/dt* increases (where *i* is the current in the stroke), and, therefore, the magnitude of the radiated electric field increases because it is dependent on *di/dt*. A narrowing of the pulse width by 10 μs can increase the magnitude of the electric field in the EMP by 30%. Uncertainty in peak current and in *di/dt* that is used in this EMP model could increase or decrease the magnitude of the radiation electric field that is responsible for ionization and attachment as it passes through the lower ionosphere. Conversely, a lengthening of the pulse could also produce a larger electric field due to constructive interference of the direct wave, the ground

reflection, and the ionospheric reflection [Cho and Rycroft, 2001]. This interference has not been accounted for in this model due to the absorbing boundary conditions used.

Another source of error may be the overall shape of the lightning current pulse. In a recent study, Frey et al. [2005] found that 50% of ISUAL-detected elves were accompanied by a lightning stroke with a β-type stepped leader. The stepped leader is one of the original stages of a lightning stroke in which a conducting path is created between cloud and ground in a number of discrete steps. The β-type stepped leaders are characterized by long, bright steps with a higher average speed than the more typical α-type stepped leader. In an electric field waveform associated with a β-type stepped leader, a series of bipolar pulses are evident about 2 to 5 ms before the return stroke [Rakov and Uman, 2003]. It is possible that this β-type leader radiation could be a factor in the total lightning EMP electron density modification. This leader activity has not been included in our approach using a simple current pulse to represent the modeled return stroke, and could be a cause of the discrepancy between the experimentally-based estimates of electron density enhancement [e.g., Cheng et al., 2007] and our modeled electron density enhancement.

These uncertainties reveal the need for more in situ measurements to better understand the many unknown quantities in this type of ionospheric research. Bearing these uncertainties in mind, it is possible that the 2D-EMP code underestimates the electron density enhancements in the lower ionosphere. However, it is still able to give a limit on the maximum electron density perturbations at given altitudes, and it describes the accumulated modifications in two-dimensional space.

Summary

We have undertaken modeling to describe the qualitative behavior of electron density enhancements at various altitudes due to the EMP generated by multiple successive lightning strokes. In this study, we have used WWLLN stroke rates as input, with the goal of extending these temporal-spatial perturbations to a global scale. These results build on previous works by providing a 2-dimensional prediction of accumulated electron density enhancements due to successive lightning EMP pulses. The model presented in this paper allows one to input realistic lightning current waveforms with realistic time separation. The results suggest that even realistic pulses and rates can produce long-lasting electron density modifications over the course of a lightning storm. But these findings also suggest that those electron density modifications will reach a limiting value over time.

The results suggest that non-linearities must be taken into account when modeling the effect of successive strokes on lower ionospheric nighttime electron densities. The non-linearity suggests that a linear approach, such as that in Rodger et al. [2001], may significantly overestimate the change in electron density at higher altitudes and underestimate it at lower altitudes, so one cannot simply add or subtract a given amount of electron density in a given location based on stroke location and strength. Instead, one must consider the stroke rate in the localized region to determine whether it is sufficient to reach the maximum limiting electron density.

The comparison between the EMP model in this paper and the results of the Cheng et al. [2007] study shows that, in general, the Cho and Rycroft [1998] model may underestimate changes in electron density for a single stroke. The study in this paper also

shows that the non-linear behavior varies by altitude: a maximum electron density limit is reached after fewer strokes for higher altitudes than for lower altitudes. In fact, the region with the most significant effect (88 km) does not reach an electron density limit for these ten strokes. However, it seems that the limiting modeled electron density profile is the same in the 83 to 91 km altitude range regardless of the initial electron density. This finding indicates that if the EMP model underestimates the change in electron density for a single stroke, this limiting electron density would be reached sooner in time than is found in this study.

This particular model could also allow one to use experimentally-measured lightning waveforms from a given storm to determine ionospheric perturbations in space and time. Future work includes validating the spatial size and magnitude of the perturbation predicted by this EMP model by using the VLF/LF short-range probing technique developed in Shao et al. [2009] and Jacobson et al. [2009].

Acknowledgements

The authors wish to thank the World Wide Lightning Location Network (http://wwlln.net), a collaboration among over 40 universities and institutions, for providing the lightning location data used in this paper.

REFERENCES

Barnum, H.B. (1999), Electromagnetic and optical characteristics of lightning measured in the Earth's ionosphere, Ph.D. thesis, Univ. of Washington, Seattle, Washington.

Barrington-Leigh, C.P. and U.S. Inan. (1999), Elves triggered by positive and negative lightning discharges. *Geophys. Res. Letters, 26*, 6, 683-686.

Chen, A. B., et al. (2008), Global distributions and occurrence rates of transient luminous events, J. Geophys. Res., 113, A08306, doi:10.1029/2008JA013101.

Cheng, Z., and S.A. Cummer (2005), Broadband VLF measurements of lightning-induced ionospheric perturbations, *Geophys. Res. Lett.,* 32, L08804, doi:10.1029/2004GL022187.

Cheng, Z., S. A. Cummer, H.-T. Su, and R.-R. Hsu (2007), Broadband very low frequency measurement of *D* region ionospheric perturbations caused by lightning electromagnetic pulses, *J. Geophys. Res.*, 112, A06318, doi:10.1029/2006JA011840.

Cho, M and M.J. Rycroft (1998), Computer simulation of the electric field structure and optical emission from cloud-top to the ionosphere, *J. of Atmos. and Solar-Terr. Phys.,* 60, 871-888.

Cho, M and M.J. Rycroft (2001), Non-uniform ionization of the upper atmosphere due to the electromagnetic pulse from a horizontal lightning discharge, *J. of Atmos. and Solar-Terr. Phys.,* 63, 559-580, doi:10.1016/S1364-6826(00)00235-2.

Cummins, K.L., M.J. Murphy, E.A. Bardo, W.L. Hiscox, R. Pyle, and A.E. Pifer (1998), Combined TOA/MDF technology upgrade of U.S. National Lightning Detection Network. *J. Geophys. Res.*, *103***,** 9035-9044.

Cummer, S.A., Inan, U.S. and Bell, T.F. (1998), Ionospheric D region remote sensing using VLF radio atmospherics. *Radio Science* **33**, pp. 1781–1792.

Dowden, R.L., J.B. Brundell, and C.J. Rodger (2002), VLF lightning location by time of group arrival (TOGA) at multiple sites. *J. Atmos. Solar-Terrest. Phys.*, *64***,** 817-830.

Ferguson, J.A., and F.P. Snyder (1987), The segmented waveguide program for long wavelength propagation calculations. Technical Document No. 1071, Naval Ocean Systems Center, San Diego, California, USA.

Fernsler, R.F. and H.L. Rowland (1996), Models of lightning-produced sprites and elves, *J. Geophys. Res.,* 101(D23), 29,653-662.

Frey, H.U., S.B. Mende, S.A. Cummer, A.B. Chen, R.R. Hsu, H.T. Su, Y.S. Chang, T. Adachi, H. Fukunishi, and Y. Takahashi (2005), Beta-type stepped leader of elve-producing lightning, *Geophys. Res. Lett.*, 32, L13824, doi:10.1029/2005GL023080.

Fukunishi, H., Y. Takahashi, M. Kubota, K. Sakanoi, U.S. Inan, W.A. Lyons (1996), Elves: Lightning-induced transient luminous events in the lower ionosphere, *Geophys. Res. Lett.*, *23*, 16, 2157-2160.

Golde, R.H. (1977), *Lightning*, Academic Press, London, UK.

Hedin, A. E. (1991), Extension of the MSIS thermospheric model into the middle and lower atmosphere, J. Geophys. Res., 96, 1159-1172.

Holzworth, R. H., M. C. Kelley, C. L. Siefring, L. C. Hale, and J. D. Mitchell (1985), Electrical measurements in the atmosphere and the ionosphere over an active thunderstorm. 2: Direct current electric fields and conductivity, J. Geophys. Res., 90, 9824–9830.

Inan, U.S., T.F. Bell, J.V. Rodriguez (1991), Heating and ionization of the lower ionosphere by lightning, *Geophys. Res. Lett., 18,* 705-708.

Jacobson, A.R., R. Holzworth, J. Harlin, R. Dowden, and E. Lay (2006), Performance Assessment of the World Wide Lightning Location Network (WWLLN), Using the Los Alamos Sferic Array (LASA) as Ground Truth, *J. Atmos. and Oceanic Technology*, *23*, 1082-1092.

Jacobson, A.R., X. M. Shao, and R. Holzworth, (2009), Full-wave reflection of lightning long-wave radio pulses from the ionospheric D-region: 1. Numerical model, *J. Geophys. Res., 114*, A03303.

Kelley, M. C., S. D. Baker, R. H. Holzworth, P. Argo, and S. A. Cummer (1997), LF and MF observations of the lightning electromagnetic pulse at ionospheric altitudes, Geophys. Res. Lett., 24(9), 1111–1114.

Lay, E. H., A. R. Jacobson, R. H. Holzworth, C. J. Rodger, and R. L. Dowden (2007), Local time variation in land/ocean lightning flash density as measured by the World Wide Lightning Location Network, J. Geophys. Res., 112, D13111, doi:10.1029/2006JD007944.

Marshall, R. A., U. S. Inan, and T. W. Chevalier (2008), Early VLF perturbations caused by lightning EMP-driven dissociative attachment, *Geophys. Res. Lett.*, 35, L21807, doi:10.1029/2008GL035358.

McRae, W.M. and N.R Thomson (2000), VLF phase and amplitude: daytime ionospheric parameters. *J. of Atmos. and Solar-Terr. Physics* **62** 7, pp. 609–618.

Mende, S.B., H.U. Frey, R.R. Hsu, H.T. Su, A.B. Chen, L.C. Lee, D.D. Sentman, Y. Takahashi, and H. Fukunishi (2005), D region ionization by lightning-induced electromagnetic pulses, *J. of Geophys. Res., 110*, A11312, doi:10.1029/2005JA011064.

Mika, A. and C. Haldoupis (2008), VLF Studies During TLE Occurrences in Europe: A Summary of New Findings, *Space Sci. Rev., 137*: 489-510, doi:10.1007/s11214-008-9382-8.

Orville, R.E. (1999), Comment on "Large peak current cloud-to-ground lightning flashes during the summer months in the contiguous United States", Monthly Weather Rev., 127, 1937-1938.

Pasko, V.P, U.S. Inan, T.F. Bell, and Y.N. Tarenenko (1997), Sprites produced by quasi-electrostatic heating and ionization in the lower ionosphere, *J. of Geophys. Res., 102*, A3, 4529-4561.

Rakov, V.A. and M.A. Uman (2003), Lightning: Physics and Effects. Cambridge University Press. Cambridge, United Kingdom.

Razier, Y.P. (1991), *Gas Discharge Physics*, Springer-Verlag, Berlin.

Rodger, C.J., O.A. Molchanov, and N.R. Thomson (1998), Relaxation of transient ionization in the lower ionosphere, *J. Geophys. Res.*, 103(A4), 6969–6975.

Rodger, C.J., M. Cho, M.A. Clilverd, and M.J. Rycroft (2001), Lower ionospheric modification by lightning-EMP: Simulation of the night ionosphere over the United States. *Geophys. Res. Lett.*, *28*(2), 199-202.

Rodger, C.J., M.A. Clilverd, N.R. Thomson, D. Nunn, and J. Lichtenberger (2005), Lightning driven inner radiation belt energy deposition into the atmosphere: regional and global estimates, *Ann. Geophys.*, 23, 3419-3430.

Rodger, C.J., S.W. Werner, J.B. Brundell, N.R. Thomson, E.H. Lay, R.H. Holzworth, and R.L. Dowden (2006), Detection efficiency of the VLF World-Wide Lightning Location Network (WWLLN): Initial case study, *Ann. Geophys.,* 24, 3197-3214.

Rodger, C.J., M.A. Clilverd, N.R. Thomson, R.J. Gamble, A. Seppälä, E. Turunen, N.P. Meredith, M. Parrot, J.A. Sauvaud, and J.-J. Berthelier (2007), Radiation belt electron precipitation into the atmosphere: recovery from a geomagnetic storm, J. Geophys. Res., 112, A11307, doi:10.1029/2007JA012383.

Rodger, C. J., J. B. Brundell, R. H. Holzworth, and E. H. Lay (2009), Growing Detection Efficiency of the World Wide Lightning Location Network, *Am. Inst. Phys. Conf. Proc., Coupling of thunderstorms and lightning discharges to near-Earth space: Proceedings of the Workshop, Corte (France),* 23.27 June 2008, 1118, 15-20, DOI:10.1063/1.3137706.

Shao X-M. and A.R. Jacobson, (2009), Model simulation of very low frequency and low frequency lightning signal propagation over intermediate ranges, *special issue on lightning, IEEE EMC Trans*, *51*, 3.

Tarenenko, Y.N., U.S. Inan, and T.F. Bell (1993), Interaction with the lower ionosphere of electromagnetic pulses from lightning: heating, attachment, and ionization, *Geophys. Res. Lett., 20,* 15, 1539-1542.

Thomas, J. N., B. H. Barnum, E. Lay, R. H. Holzworth, M. Cho, and M. C. Kelley (2008), Lightning-driven electric fields measured in the lower ionosphere: Implications for transient luminous events, J. Geophys. Res., 113, A12306, doi:10.1029/2008JA013567.

Thomson, N.R. (1993), Experimental daytime VLF ionospheric parameters. *Journal of Atmospheric and Terrestrial Physics* **55** 2, pp. 173–184.

Verronen, P.T., A. Seppälä, M.A. Clilverd, C.J. Rodger, E. Kyrölä, C.F. Enell, T. Ulich, and E. Turunen (2005), Diurnal variation of ozone depletion during the October–November 2003 solar proton events, *J. Geophys. Res.,* 110, A09S32, doi:10.1029/2004JA010932.

Wait, J.R. and K.P. Spies (1964), Characteristics of the Earth-Ionosphere Waveguide for VLF Radio Waves, *Nat. Bureau of Standards Tech. Notes*, 300, Washington, DC.

Figure Captions

Figure 1. Numerically-calculated 1/*e* decay times for electron density enhancement versus altitude.

Figure 2. Initial, or steady-state, electron density profile (right side), along with the electron density profile 2 ms after one 150-kA stroke (top panel) and 2 ms after ten 150-kA strokes (bottom panel) spaced 5 seconds apart.

Figure 3. Percentage change in electron density from steady-state 2 ms after one 150 kA stroke (top panel) and 2 ms after ten 150 kA strokes (bottom panel). White contours represent 0 percent change. The maximum contour level show in the top panel is 30 percent change and in the bottom panel is 250 percent change. The minimum contour level shown in the bottom panel is -50 percent change.

Figure 4. Electron density at 92, 90, 88, and 85 km altitude after each successive stroke using the non-linear technique (solid line) versus a linear technique (dashed-dotted line).

Figure 5. Percent change in electron density for 92, 90, 88, 85 km altitude after each successive stroke.

Figure 6. Perturbed electron density profile taken vertically at the range of maximum percentage change after a) 1 stroke and b) 10 strokes for 2 initial electron density profiles (solid and dotted lines). Thin solid lines represent initial electron density profiles.

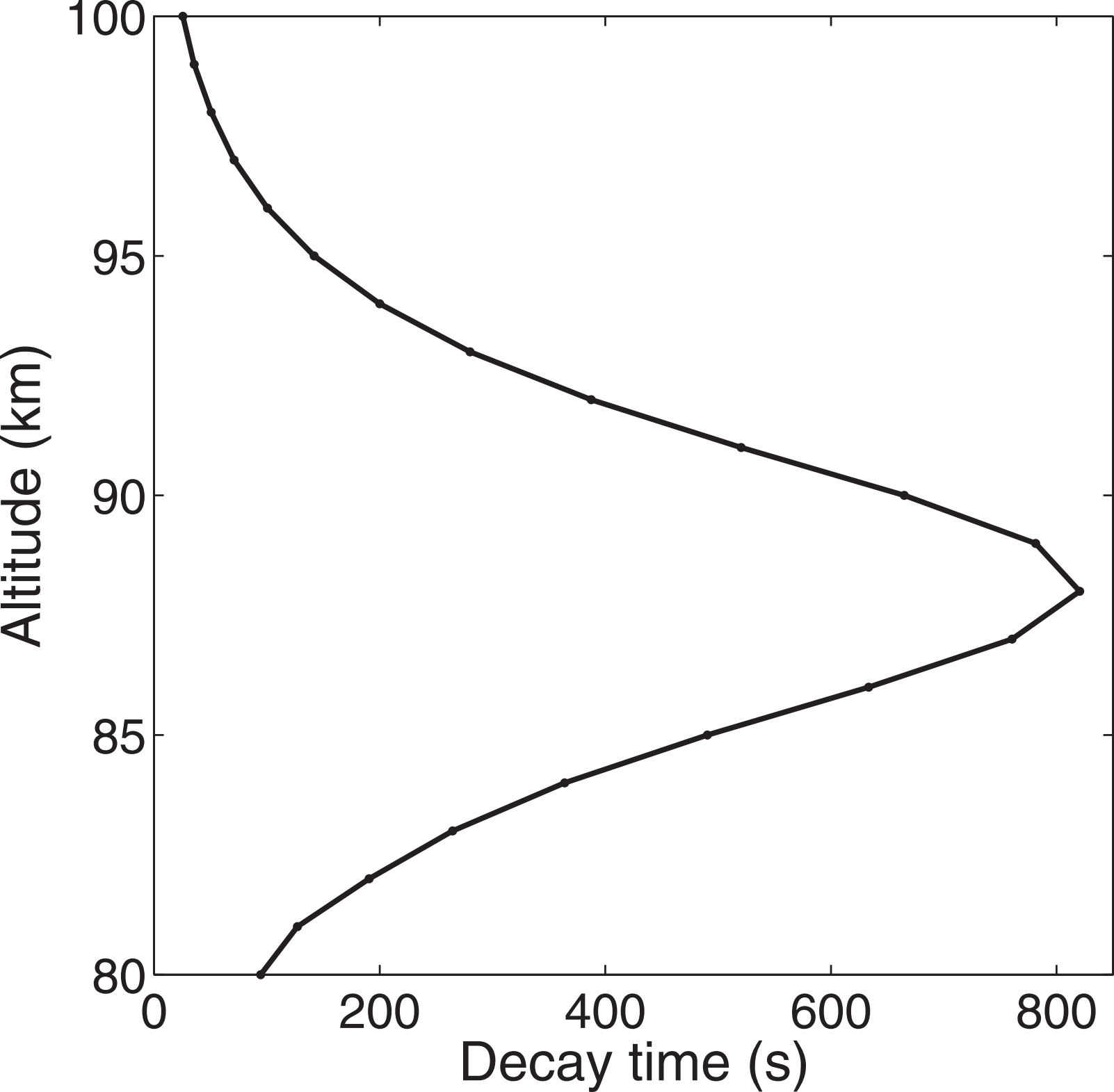
100
95
90
85
80
Altitude (km)
0
200
400
600
800
Decay time (s)

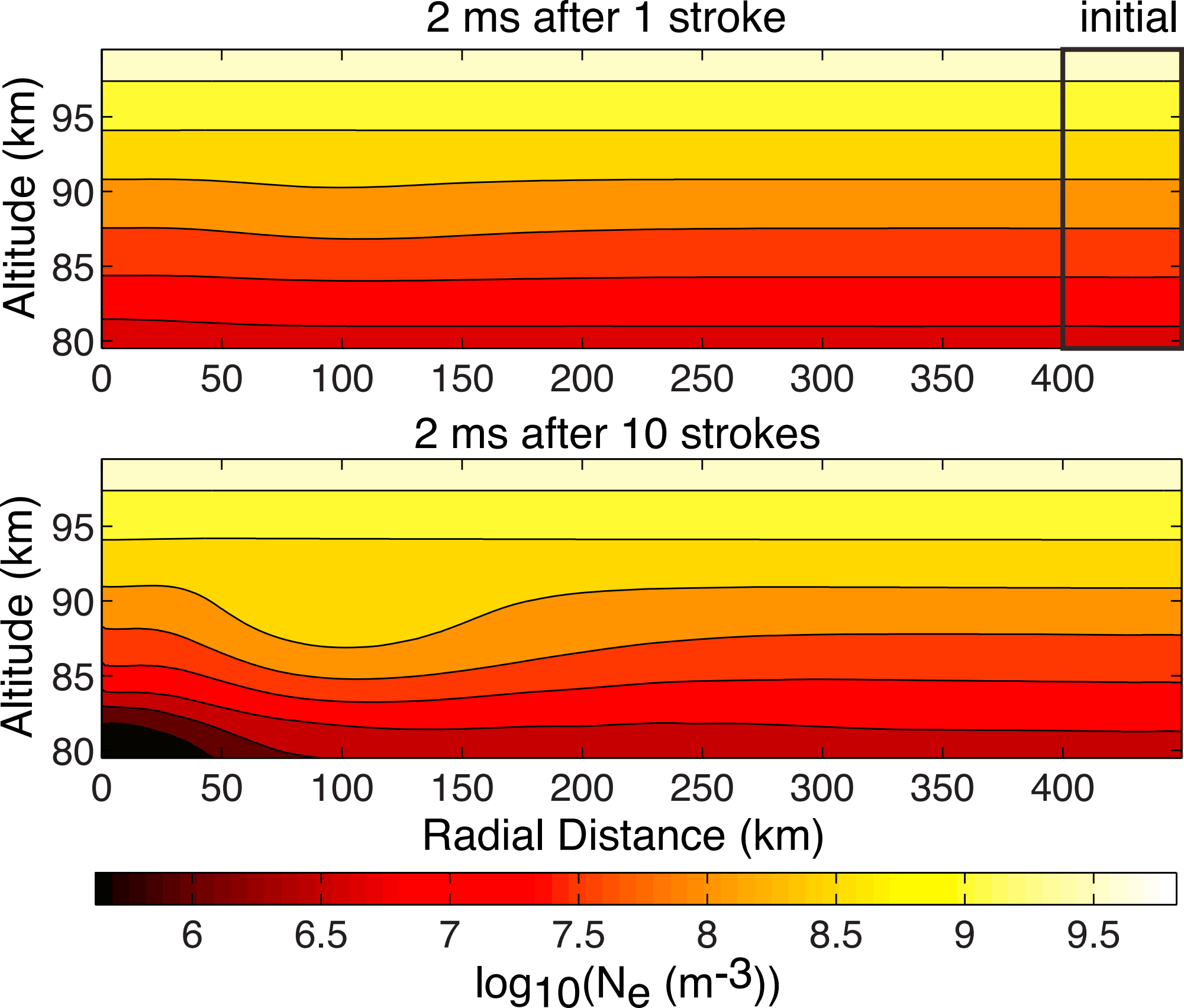
2 ms after 1 stroke
initial
Altitude (km)
95
90
85
80
0
50
100
150
200
250
300
350
400
2 ms after 10 strokes
Altitude (km)
95
90
85
80
0
50
100
150
200
250
300
350
400
Radial Distance (km)
6
6.5
7
7.5
8
8.5
9
9.5
log10(Ne (m-3))

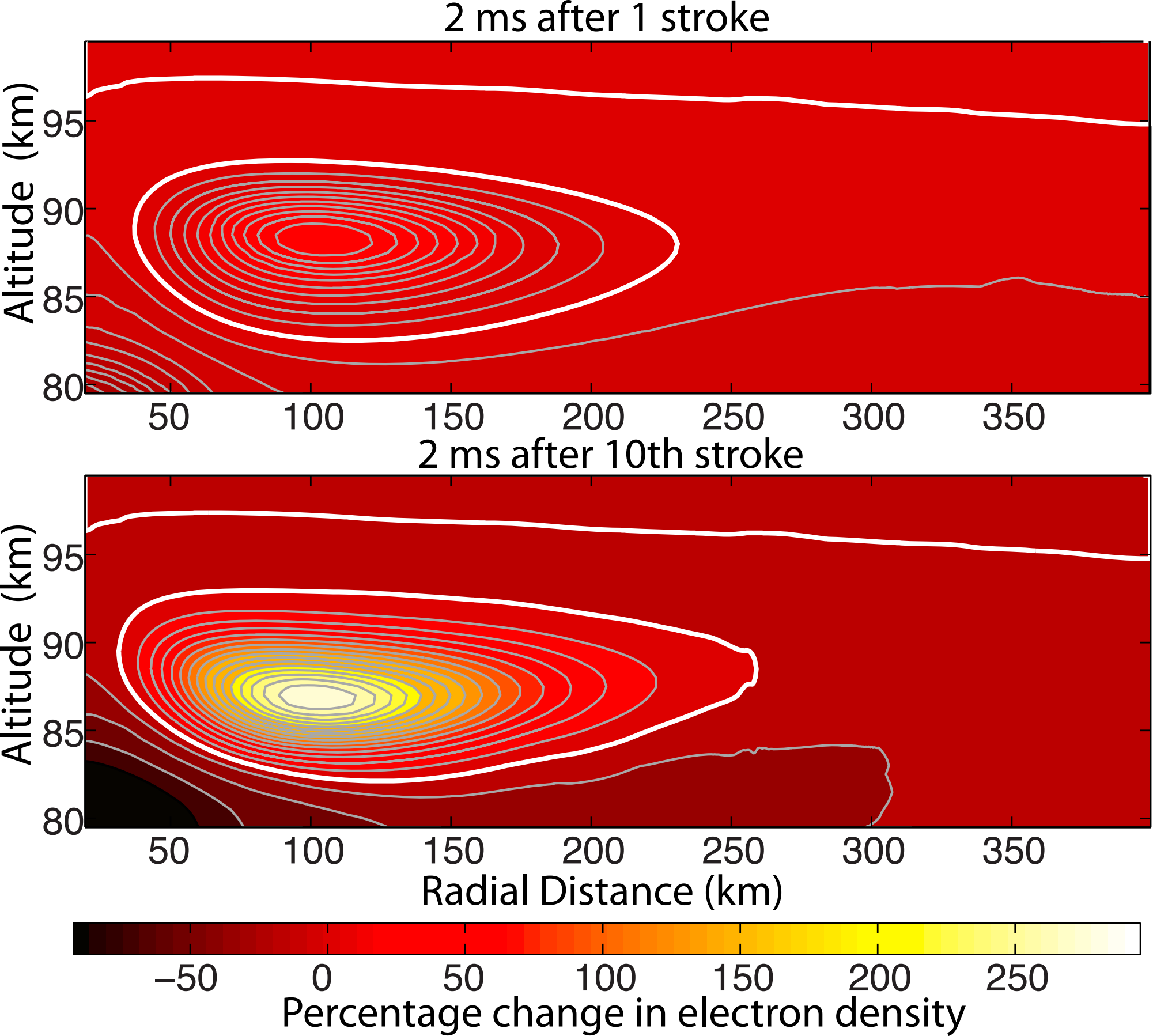
2 ms after 1 stroke
Altitude (km)
95
90
85
80
50
100
150
200
250
300
350
2 ms after 10th stroke
Altitude (km)
95
90
85
80
50
100
150
200
250
300
350
Radial Distance (km)
−50
0
50
100
150
200
250
Percentage change in electron density

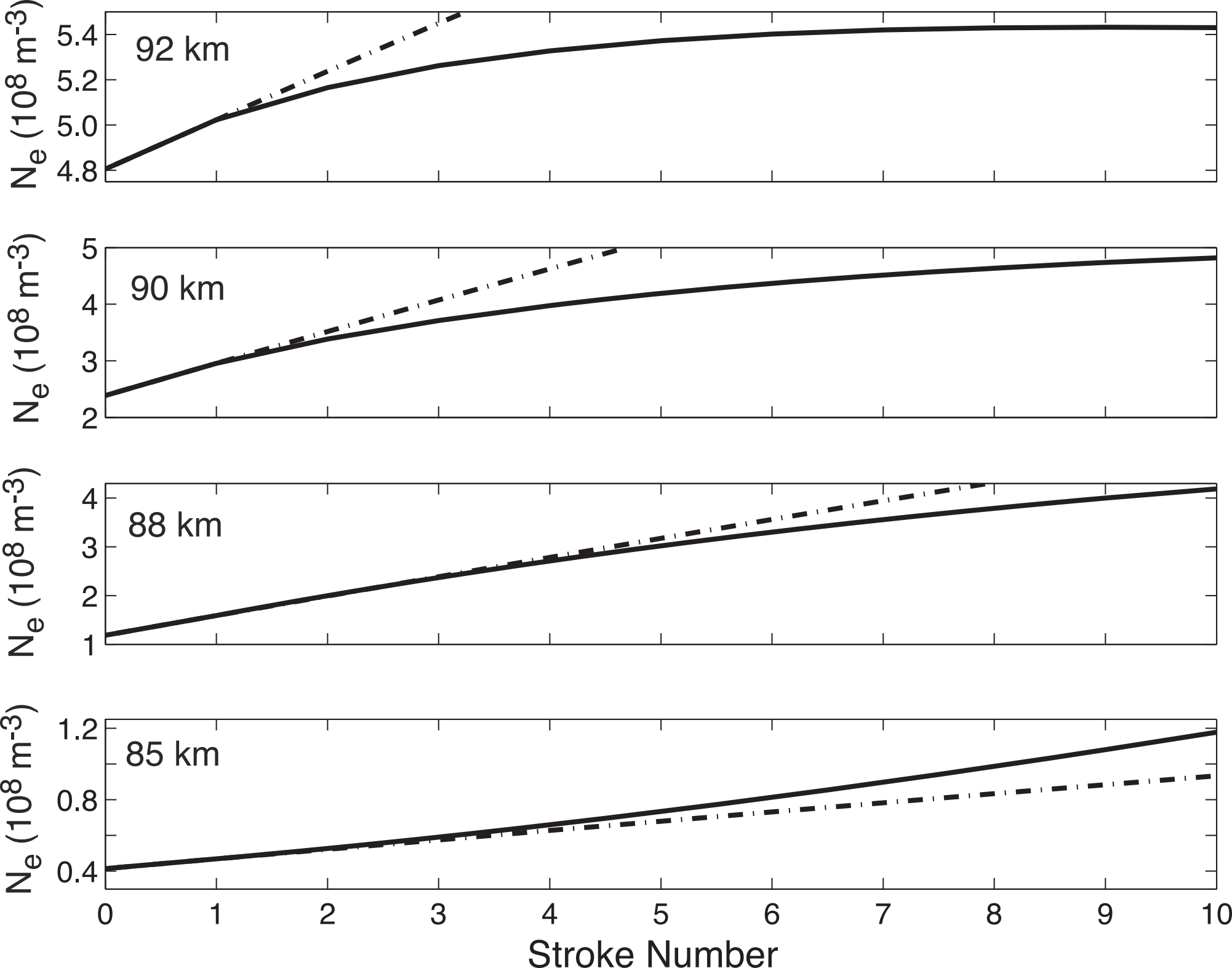
92 km
90 km
88 km
85 km
N_e (10^8 m^{-3})
Stroke Number
0
1
2
3
4
5
6
7
8
9
10
4.8
5.0
5.2
5.4
2
3
4
5
1
2
3
4
0.4
0.8
1.2

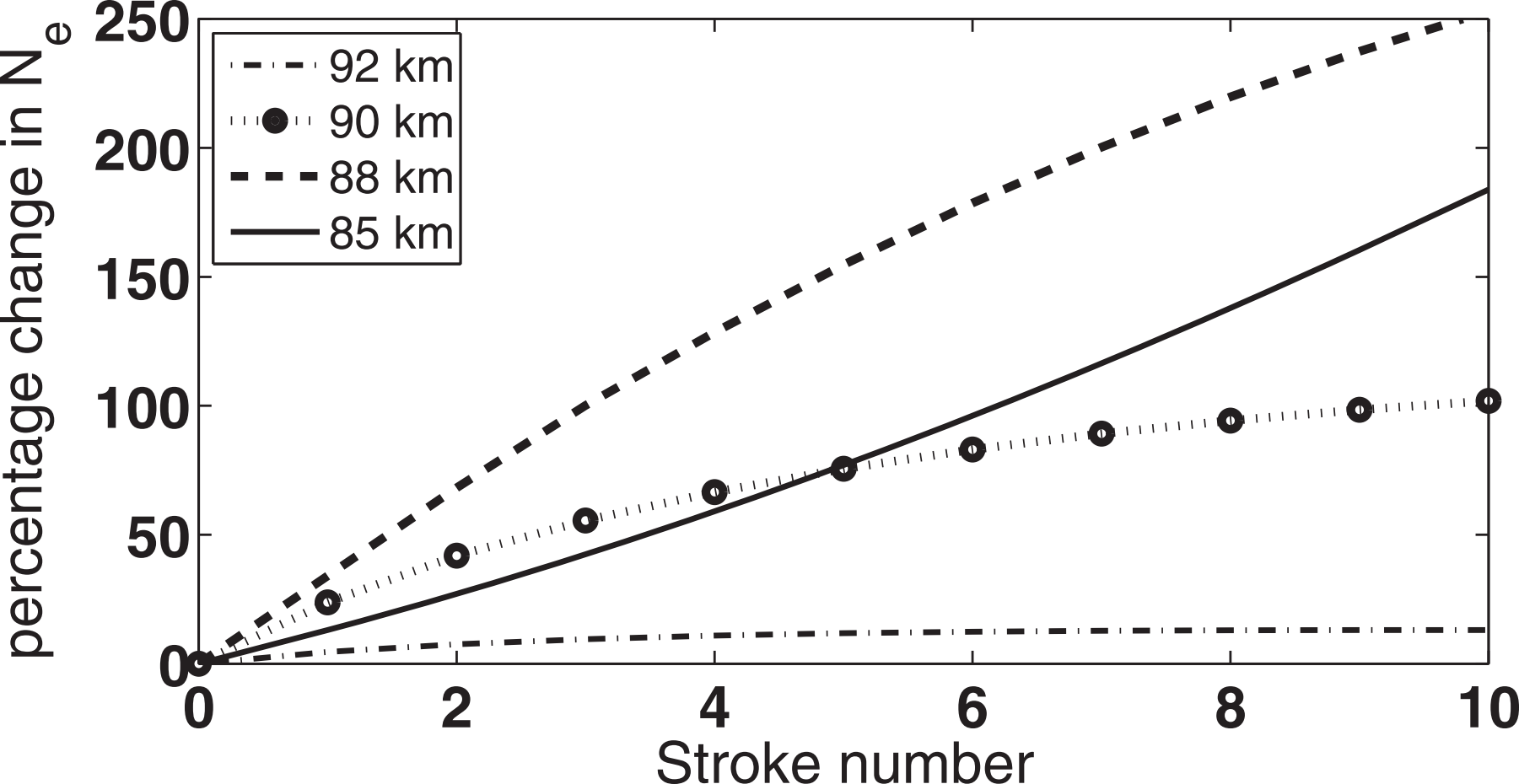
92 km
90 km
88 km
85 km
percentage change in N_e
250
200
150
100
50
0
0
2
4
6
8
10
Stroke number

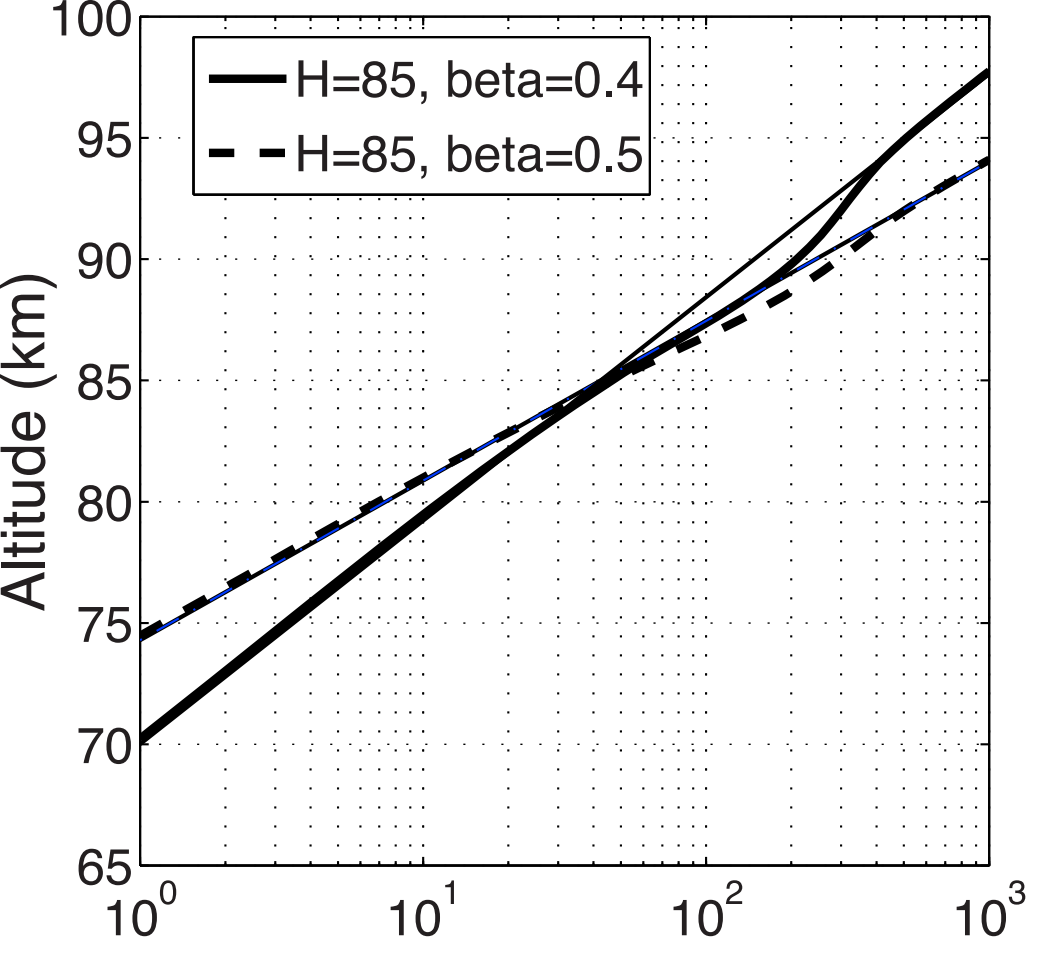
H=85, beta=0.4
H=85, beta=0.5
Altitude (km)
100
95
90
85
80
75
70
65
10^0
10^1
10^2
10^3

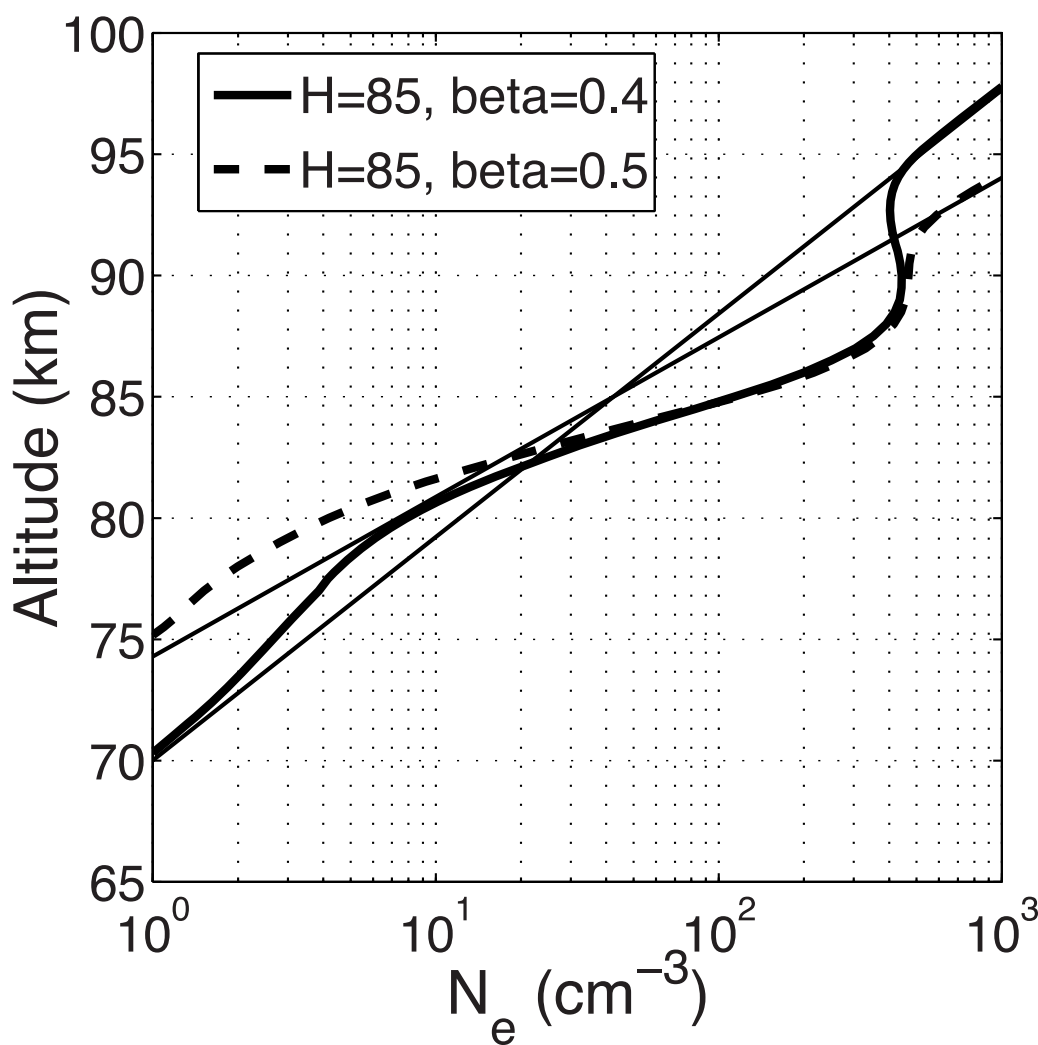
H=85, beta=0.4
H=85, beta=0.5
Altitude (km)
100
95
90
85
80
75
70
65
10^0
10^1
10^2
10^3
N_e (cm^{-3})